Molecular Biology of the Cell
Vol. 16, 2799–2808, June 2005

The Prion Protein and Its Paralogue Doppel Affect Calcium Signaling in Chinese Hamster Ovary Cells

Marisa Brini,*† Manuela Miuzzo,* Nicola Pierobon,* Alessandro Negro,*† and Maria Catia Sorgato*

*Department of Biological Chemistry, University of Padova, CNR Institute of Neuroscience and CRIBI, 35121 Padova, Italy; and †Department of Experimental Veterinary Sciences, University of Padova, 35020 Legnaro-Padova, Italy

Submitted October 21, 2004; Revised March 2, 2005; Accepted March 16, 2005
Monitoring Editor: Thomas Fox

The function of the prion protein (PrP^c), implicated in transmissible spongiform encephalopathies (TSEs), is largely unknown. We examined the possible influence of PrP^c on Ca^{2+} homeostasis, by analyzing local Ca^{2+} fluctuations in cells transfected with PrP^c and Ca^{2+}-sensitive aequorin chimeras targeted to defined subcellular compartments. In agonist-stimulated cells, the presence of PrP^c sharply increases the Ca^{2+} concentration of subplasma membrane Ca^{2+} domains, a feature that may explain the impairment of Ca^{2+}-dependent neuronal excitability observed in TSEs. PrP^c also limits Ca^{2+} release from the endoplasmic reticulum and Ca^{2+} uptake by mitochondria, thus rendering unlikely the triggering of cell death pathways. Instead, cells expressing Doppel, a PrP^c paralogue, display opposite effects, which, however, are abolished by the coexpression of PrP^c. These findings are consistent with the functional interplay and antagonistic role attributed to the proteins, whereby PrP^c protects, and Doppel sensitizes, cells toward stress conditions.

INTRODUCTION

The cellular prion protein (PrP^c) is a highly conserved cell surface glycoprotein, particularly expressed in the CNS with a still unrecognized function. A conformationally modified isoform (PrP^{Sc}) of PrP^c is the major component of prions, the etiological agent at the basis of fatal neurodegenerative disorders, called transmissible spongiform encephalopathies (TSEs). TSEs present as sporadic, genetic, and infectious illnesses, and include Creutzfeldt-Jakob disease (CJD) in humans, and bovine spongiform encephalopathy in cattle (Prusiner, 1998).

The mechanism of PrP^c conversion into PrP^{Sc} is not yet elucidated, nor it is clear if the disease progression relates to PrP^{Sc} toxic effect, or to the deprivation of PrP^c functionality. The most prominent evidence in support of the former hypothesis is that most PrP-knockout mice remain viable, and do not develop spontaneous neurodegeneration (Bueler *et al.,* 1992; Manson *et al.,* 1994), even if the PrP^c gene is postnatal deleted (Mallucci *et al.,* 2002). An essential role of PrP^c in cell survival comes, however, from the finding that wild-type PrP transgenes abrogate the cerebellar degeneration and late-onset ataxia developed by some PrP-knockout lines over expressing a protein, named Doppel (Dpl; Sakaguchi *et al.,* 1996; Li *et al.,* 2000; Moore *et al.,* 1999, 2001; Rossi *et al.,* 2001). Dpl is normally absent in the CNS of adult animals and resembles truncated PrP^c; it lacks the copper-binding N-terminus (Brown *et al.,* 1997) and is structurally and biochemically similar to PrP^c carboxyl end (Silverman *et al.,* 2000; Mo *et al.,* 2001). Also the role of Dpl in the CNS is obscure, but the capacity of PrP^c to restore the normal phenotype of Dpl-over expressing mice has suggested that PrP^c and Dpl have antagonistic functions and that PrP^c suppresses a death signal triggered by Dpl.

Comparative studies using cells from wild-type or PrP-knockout animals or infected by prions also argue in favor of "the-loss-of-function hypothesis," suggesting that PrP^c protects cells by controlling the copper metabolism governing the cell resistance to oxidative stress (Brown *et al.,* 2002) or by playing an antiapoptotic role (reviewed in Hetz *et al.,* 2003a). Importantly, other data from electrophysiologic studies, and/or cell Ca^{2+} measurements, converge in supporting that PrP^c absence, or its recruitment into prions, leads to a compromised Ca^{2+} homeostasis and that such a defect ultimately impinges on a few Ca^{2+}-dependent neurophysiologic functions, such as plasma membrane K^+ currents, after-hyperpolarization potential (AHP) and depolarizing after-potential (DAP) events (Jefferys *et al.,* 1994; Colling *et al.,* 1996; Johnston *et al.,* 1998; Barrow *et al.,* 1999; Herms *et al.,* 2000, 2001; Mallucci *et al.,* 2002).

Yet, if PrP^c is involved in the correct handling of cell Ca^{2+}, the above-reported findings are hardly surprising, given that Ca^{2+} is an ubiquitous intracellular messenger regulating a large amount of cell functions and that subtle alterations of endoplasmic reticulum (ER) and mitochondrial

This article was published online ahead of print in *MBC in Press* (http://www.molbiolcell.org/cgi/doi/10.1091/mbc.E04–10–0915) on March 23, 2005.

Address correspondence to: Maria Catia Sorgato (catia.sorgato@unipd.it).

Abbreviations used: AEQ, aequorin; cytAEQ, erAEQ, mtAEQ, and pmAEQ, aequorin targeted to the cytosol, the endoplasmic reticulum, the mitochondrial matrix and the plasma membrane, respectively; tBuBHQ, 2,5-di-(*tert*-butyl)-1,4-benzohydroquinone; CCE, capacitative Ca^{2+} entry; Dpl, Doppel; Dpl_{rec}, recombinant Doppel; ER, endoplasmic reticulum; GFP, green fluorescent protein; GPI, glycosylphosphatidylinositol; $InsP_3$, inositol-1,4,5-triphosphate; mAb, monoclonal antibody; PrP^c, cellular prion protein; PrP^{Sc}, pathological isoform of prion protein; PrP_{rec}, recombinant prion protein; SERCA, sarco(endo)plasmic reticulum Ca^{2+}-ATPase; SOCC, store-operated Ca^{2+} channels; TSE, transmissible spongiform encephalopathy.

Ca^{2+} pools control initiation of cell death pathways. For example, both overload and depletion of the ER Ca^{2+} concentration ($[Ca^{2+}]$) can impinge on correctly folded protein levels, thereby inducing (ER−) stress responses that may determine apoptosis (Orrenius *et al.*, 2003). Accordingly, perturbed ER Ca^{2+} regulation contributes to neuronal degeneration (reviewed in Mattson *et al.*, 2000; Paschen, 2001), including Alzheimer's disease and TSEs (Nakagawa *et al.*, 2000; Hetz *et al.*, 2003b). Also mitochondrial Ca^{2+} fluxes are integrated modulators of the cell Ca^{2+} signaling and intimately govern the cell fate. Indeed, mitochondria respond to high $[Ca^{2+}]$ microdomains that form in proximity of plasma membrane, and/or sarco/endoplasmic reticulum, Ca^{2+} channels upon cell stimulation (Brini, 2003). By activating the production of ATP, such a relayed signal satisfies immediate physiological energy demands (Jouaville *et al.*, 1999). However, it can also turn into a death signal, given that excessive Ca^{2+} accumulation triggers abnormal mitochondrial membrane permeability (Bernardi, 1999) and release of proapoptotic factors to the cytoplasm (Li *et al.*, 1997).

In view of the many implications related to the fine tuning of local Ca^{2+} changes, we have investigated on the involvement of PrP^c in Ca^{2+} homeostasis, using CHO cells transiently transfected with PrP^c and the recombinant Ca^{2+}-sensitive photoprotein aequorin (AEQ) targeted to specific cell compartments. Furthermore, within the proposed functional antagonism of PrP^c and Dpl, we also monitored the Ca^{2+} metabolism in AEQ-transfected cells over expressing Dpl, either alone or together with PrP^c.

MATERIALS AND METHODS

Expression Plasmids

PrP^c and Dpl isoforms used in all experiments were the murine (m) and human (h) ones, respectively. The expression vector for eukaryotic cells containing the coding sequence for hDpl was constructed as in Massimino *et al.* (2004), whereas that coding for $mPrP^c$ was constructed using a mouse genomic DNA as template, and by *Prnp* amplification by PCR with primers 5′ GCGCTAGCATGGCGAACCTTGGCTACTGGCTGC 3′; and 5′ CGGAATTCATCCCACGATCAGGAAGATGAG 3′. Amplified products were cut at *Nhe*I and *Eco*RI sites and cloned directly in the phEGFP plasmid (Clontech, Palo Alto, CA) between the same restriction sites to obtain plasmid pcDNAmPrP. To express $mPrP^c$ carrying the epitope specific for monoclonal antibody (mAb) 3F4, L108M, and V111M point mutations were introduced in pcDNAmPrP by inverse PCR, using primers 5′ CATATGGCAGGGGCTGCGGCAGCTGGGC 3′ and 5′ CTTCATGAAGGTTTTTGGTTTGCTGGGCT 3′. The amplified product was itself ligated after T4 polynucleotide kinase treatment, to yield plasmid pmPrP3F4. The expression plasmid for the fusion protein between the green fluorescent protein (GFP) and the glycosylphosphatidylinositol (GPI) attachment signal of bovine PrP^c (GFP-GPI_{PrP}) was as described in Cereghetti *et al.* (2004), whereas plasmids for the photoprotein AEQ targeted to the various cell compartments were obtained according to Brini *et al.* (1995) for cytAEQ; Montero *et al.* (1995, 2000) for erAEQ; Marsault *et al.* (1997) for pmAEQ; and Rizzuto *et al.* (1992) for mtAEQ. Recombinant (rec) mPrP (23–230; containing the mAb 3F4 epitope) was generated in, and purified from *Escherichia coli*, following the method described in Negro *et al.* (2000) for the bovine PrP isoform, whereas $hDpl_{rec}$ (28–152) was obtained as in Cereghetti *et al.* (2004).

Cell Cultures and Transfection

Experiments were carried out with CHO cells, cultured in 75-cm^2 flasks (37°C, 5% CO_2 atmosphere), using Ham's F12 medium (EuroClone, Devon, United Kingdom) supplemented with 10% fetal calf serum (FCS), penicillin (100 U/ml), and streptomycin (100 μg/ml). The cells, seeded onto glass coverslips at 4.5×10^4 and 3.5×10^5 cells/cm^2 for fura-2 and aequorin measurements, respectively, were transiently transfected preferentially with the Lipofectamine Plus reagent (Invitrogen, Milano, Italy), following manufacturer's instructions (in double and triple transfection experiments the quantity of each added plasmid was proportionally reduced). To optimize PrP^c and Dpl expression, 6 h after transfection the medium was changed, and cells were kept at 30°C for 48 h before fura-2-, or aequorin-based, Ca^{2+} measurements, or immunolabeling assays. Importantly, identical results were obtained when cells were transfected using the Ca^{2+} phosphate-based procedure (Rizzuto *et al.*, 1995) and a total amount of 3 μg of plasmid DNA (1.5:1.5 μg in the case of double transfection). To generate CHO cells stably expressing $mPrP^c$, the method was as described in Massimino *et al.* (2004).

Immunocytochemistry, Western Blotting, and Densitometric Analysis

Immunocytochemistry and image analysis of intact cells, immunoblotting, and densitometric analyses were carried out as in Negro *et al.* (2001) and Massimino *et al.* (2004), except that 20 μg of cell lysates were loaded in each gel lane.

Antibodies

For immunocytochemistry and immunoblotting of PrP^c and Dpl, the following antibodies were used (dilutions are given in parenthesis): anti-PrP mAb 8H4, raised against the human PrP 173–185 sequence (a kind gift of Dr. M.S. Sy, Case Western University, Cleveland, OH; 1/300 for immunolocalization; 1/8000 for immunoblotting), or mAb 3F4 (DAKO, Glostrup, Denmark; 1/100 for immunolocalization; 1/1000 for immunoblotting), which gave the same results as with mAb 8H4; and anti-Dpl mAb Dpl-79 (kindly provided by Dr. J. Grassi, Commissariat a l'Energie Atomique, Saclay, France) raised against $hDpl_{rec}$ (28–152; 1/100 for immunolocalization; 1/1000 for immunoblotting). The immunoblotting of the sarco(endo)plasmic reticulum Ca^{2+}-ATPase (SERCA) and β-actin was carried out using commercially available mAbs against the ubiquitous isoform (SERCA2; clone IID8, Affinity Bioreagents, Golden, CO; 1/1000), and β-actin (Sigma, St. Louis, MO; 1/4000), respectively, and anti-calreticulin polyclonal antibody (Affinity Bioreagents; 1/1000) was used for calreticulin immunolabelings.

Ca^{2+} Measurements: Aequorin

Although the cytAEQ plasmid coded for the wild-type AEQ, to reduce the affinity for Ca^{2+}, erAEQ, mtAEQ, and pmAEQ plasmids expressed aequorins carrying a mutation in one Ca^{2+} binding site (Montero *et al.*, 1995). Functional erAEQ was reconstituted with a modified prosthetic group (coelenterazine n, Molecular Probes, Eugene, OR), after depleting ER Ca^{2+} (Montero *et al.*, 1995; Barrero *et al.*, 1997). To this end, cells were incubated (1 h, 4°C) in KRB (Krebs-Ringer modified buffer: 125 mM NaCl, 5 mM KCl, 1 mM Na_3PO_4, 1 mM $MgSO_4$, 5.5 mM glucose, 20 mM HEPES, pH 7.4) supplemented with ionomycin (5 μM), EGTA (600 μM), and coelenterazine n (5 μM). After extensive washings with KRB containing 2% bovine serum albumin and 1 mM EGTA, the coverslip with the cells was transferred to the thermostatted (37°C) chamber of a purpose-built luminometer. Conversely, transfected cytAEQ, mtAEQ, and pmAEQ were reconstituted by incubating cells (1–3 h, 37°C, 5% CO_2 atmosphere) with wild-type coelenterazine (5 μM, Molecular Probes) in DMEM containing 1% FCS. Measurements started by perfusing cells with KRB supplemented with 1 mM $CaCl_2$. Alternatively, pmAEQ was reconstituted in cells incubated with coelenterazine in KRB containing EGTA (100 μM). In this case, experiments started with cells in the EGTA-supplemented KRB, which was then replaced by $CaCl_2$ (1 mM)-containing KRB. Other additions were as specified in the figures. Experiments ended by lysing cells with digitonin (100 μM) in a hypotonic Ca^{2+}-rich solution (10 mM $CaCl_2$ in H_2O), to discharge the remaining aequorin pool. The light signal was collected and stored in an IBM-compatible computer for further analyses. Aequorin luminescence data were calibrated off-line into $[Ca^{2+}]$ values, using a computer algorithm based on the Ca^{2+} response curve of wild-type and mutant aequorins, as previously described (Brini *et al.*, 1995).

Fura-2

Cells, cotransfected with the phEGFP plasmid (Clontech) and either PrP^c or Dpl, were loaded with fura-2 AM (5 μM, Molecular Probes) as in Malgaroli *et al.* (1987), and the coverslip was then placed on the stage of a Zeiss Axiovert 100 epifluorescence microscope (Göttingen, Germany), equipped with a 16-bit digital CCD videocamera (Micromax, Princeton Instruments, Trenton, NJ). Samples were alternately illuminated at 340 and 380 nm, and the emitted light (filtered with an interference filter centered at 510 nm) was collected by the camera. Images were acquired using the Metafluor software (Universal Imaging, West Chester, PA). The ratio values (1 ratio image/s) were calculated off-line, after background subtraction from each single image.

Statistical Analysis

Data are reported as means ± SD; n indicates the number of experiments. Statistical differences were evaluated by Student's two-tailed *t* test for impaired samples, with a *p* value lower than 0.05 being considered statistically significant.

RESULTS

Localization and Expression of Transiently Transfected PrP^c or Dpl

Before analyzing whether PrP^c, or Dpl, affects Ca^{2+} homeostasis, we ascertained their correct cell distribution by

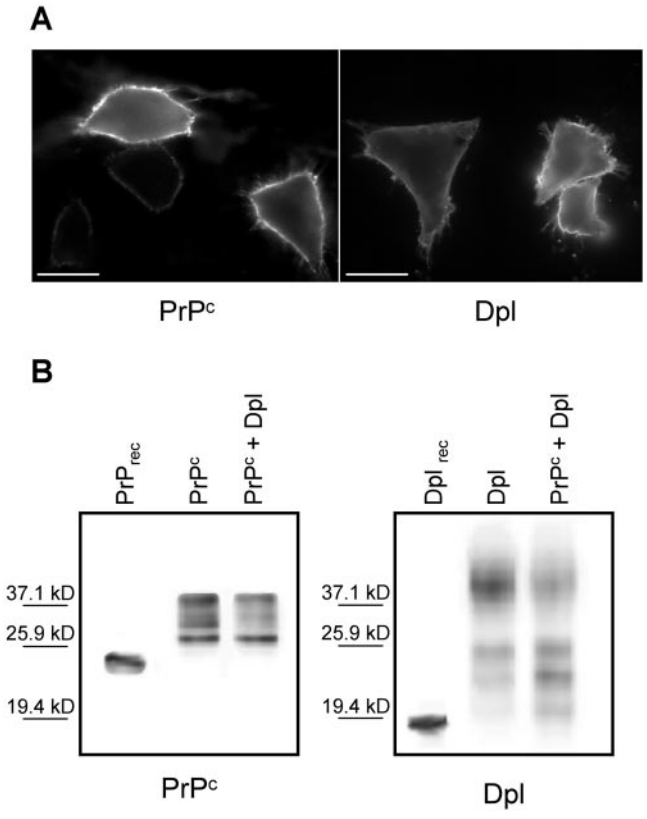

Figure 1. Localization (A) and expression level (B) of PrP^c and Dpl in transiently transfected CHO cells. (A) Distribution of PrP^c and Dpl in intact cells expressing each protein alone, after treatment (4°C) with anti-PrP mAb 8H4 (left), or anti-Dpl mAb Dpl-79 (right), followed by fluorescein isothiocyanate-conjugated secondary antibody. Both proteins are present on the cell surface, correctly exposed to the exoplasmic space. Bar, 20 μm. (B) Western blots of PrP^c (left) and Dpl (right) of cells expressing each protein alone (second lanes), or together (third lanes), show that both proteins exhibit high mass diffuse bands typical of their complex N-linked glycosylation (Massimino *et al.,* 2004). Cell lysate SDS-PAGE separated proteins were immunoblotted with the above-described mAbs, and immunoreactive bands were then subjected to densitometric analysis. Comparison between the density of PrP^c- and Dpl-containing bands and the band density elicited by a known quantity of PrP_{rec} or Dpl_{rec} (0.5 ng, first lane of the left and right panel, respectively) yielded a value of 3.8 and 4.0 ng (in singly transfected cells, second lanes of both panels), and 2.1 and 2.3 ng (in doubly transfected cell, third lanes of both panels) for PrP^c and Dpl amounts, respectively.

immunostaining CHO cells transiently transfected with either PrP^c or Dpl. As evident from the uniform labeling of the plasma membrane (Figure 1A), obtained by adding (4°C) anti-PrP-, or anti-Dpl-, mAbs to intact cells, PrP^c and Dpl are exposed to the exoplasmic space, in accord with the presence of a GPI anchor in both proteins, and with similar data reported previously (Massimino *et al.,* 2004). Using dual-labeling immunocytochemistry, an identical localization of the proteins to the cell surface was observed in cells expressing PrP^c, or Dpl, together with the AEQ probes, and in those cotransfected with both PrP^c and Dpl (see also Massimino *et al.,* 2004; unpublished data). Figure 1B (second lanes), reporting the immunoblots of PrP^c and Dpl in cells housing each protein alone, shows that the two cell types express similar protein amounts. Importantly, by applying immunocytochemistry and Western blot techniques to untransfected CHO cells, we found that no endogenous PrP^c, or Dpl, was detectable over the entire experimental time period.

ER Ca^{2+} in PrP^c- or Dpl-expressing Cells

The ER is the main Ca^{2+} storage of the cell as it houses Ca^{2+}-binding proteins and SERCA pumps that transport Ca^{2+} against a high concentration gradient. To measure the ER luminal $[Ca^{2+}]$ ($[Ca^{2+}]_{er}$), we used erAEQ that targets exclusively to this compartment (Montero *et al.,* 1995). To function as a Ca^{2+} probe, recombinant AEQ needs to be reconstituted in the active complex with its prosthetic group, coelenterazine; added to cells, coelenterazine permeates the cell membranes and combines efficiently with AEQ. However, to avoid the instantaneous consumption of the holophotoprotein by the high luminal $[Ca^{2+}]_{er}$, erAEQ-containing cells had to be first reduced in the ER Ca^{2+} content (by adding the Ca^{2+} ionophore ionomycin in the absence of external Ca^{2+}) before reconstitution (in a Ca^{2+}-free medium) with coelenterazine n, which is modified so as to reduce the Ca^{2+} affinity of AEQ (Barrero *et al.,* 1997).

Figure 2A reports ER Ca^{2+} measurements in parallel batches of cells transiently expressing erAEQ alone (control cells, light gray trace) or together with PrP^c (black trace) or Dpl (dark gray trace). In agreement with previous reports (Brini *et al.,* 2000), ~1 min after adding $CaCl_2$ (1 mM), the $[Ca^{2+}]_{er}$ of control cells reached a steady state level close to 400 μM (390 ± 20 μM, n = 15). This value, however, is ~15% lower than that observed in the presence of PrP^c, or Dpl, which was 455 ± 20 μM (n = 15) and 460 ± 20 μM (n = 15), respectively. Importantly, unless an ER Ca^{2+}-discharging stimulus was applied, in all cases the shown Ca^{2+} plateau levels were stably maintained (unpublished data) and thus well represent the uppermost free Ca^{2+} amount that the three cell types can accumulate in the ER.

Next, we examined cells for the capacity to release Ca^{2+} after the addition of ATP (100 μM) at the indicated time point (Figure 2A). By activating plasma membrane P2Y receptors coupled to Gq proteins and phospholipase C, ATP induces the generation of inositol-1,4,5-triphosphate ($InsP_3$), which promotes the discharge of the ER Ca^{2+} stores through the channel activity of $InsP_3$ receptors ($InsP_3Rs$; Streb *et al.,* 1983). Obtained results clearly demonstrate that the dynamics of Ca^{2+} efflux differs in the three cell types. The largest Ca^{2+} discharge occurs in the presence of Dpl (dark gray trace), so that the remaining $[Ca^{2+}]_{er}$ (130 ± 20 μM, n = 9) is less than in PrP^c-containing cells (black trace; 215 ± 20 μM, n = 7), whereas it equals that of controls (light gray trace; 110 ± 20 μM, n = 9; note, however, the lower starting $[Ca^{2+}]_{er}$ in the latter cells). Yet differences regard also the kinetics of the process, in that the fastest value is exhibited by Dpl-expressing cells, whereas the rate rapidly slows down in cells with PrP^c (velocity at half maximal Ca^{2+} discharge $[V_{1/2}]$: 27 ± 3 μM/s, n = 5, in cells with Dpl; 18 ± 1 μM/s, n = 5, in cells with PrP^c; 20 ± 2 μM/s, n = 5, in controls). Intriguingly, however, after ~30–40 s from the maximal Ca^{2+} depletion and in the continuous presence of the agonist, a partial refilling of ER stores occurred in Dpl-containing cells, whereby the final $[Ca^{2+}]_{er}$ plateau settled to a value (210 ± 30 μM, n = 9), closely approximating that observed with PrP^c.

Notably, we could exclude that the peculiar ER Ca^{2+} handling in cells with PrP^c, or Dpl, is the consequence of the double transfection protocol (i.e., PrP^c, or Dpl, associated with erAEQ), given that cells coexpressing erAEQ and a non-natural GPI-linked protein (GFP-GPI_{PrP}, made of GFP fused to the GPI-attachment signal of PrP^c), have the same behavior of controls (Figure 2B). Nor did PrP^c, or Dpl, alter

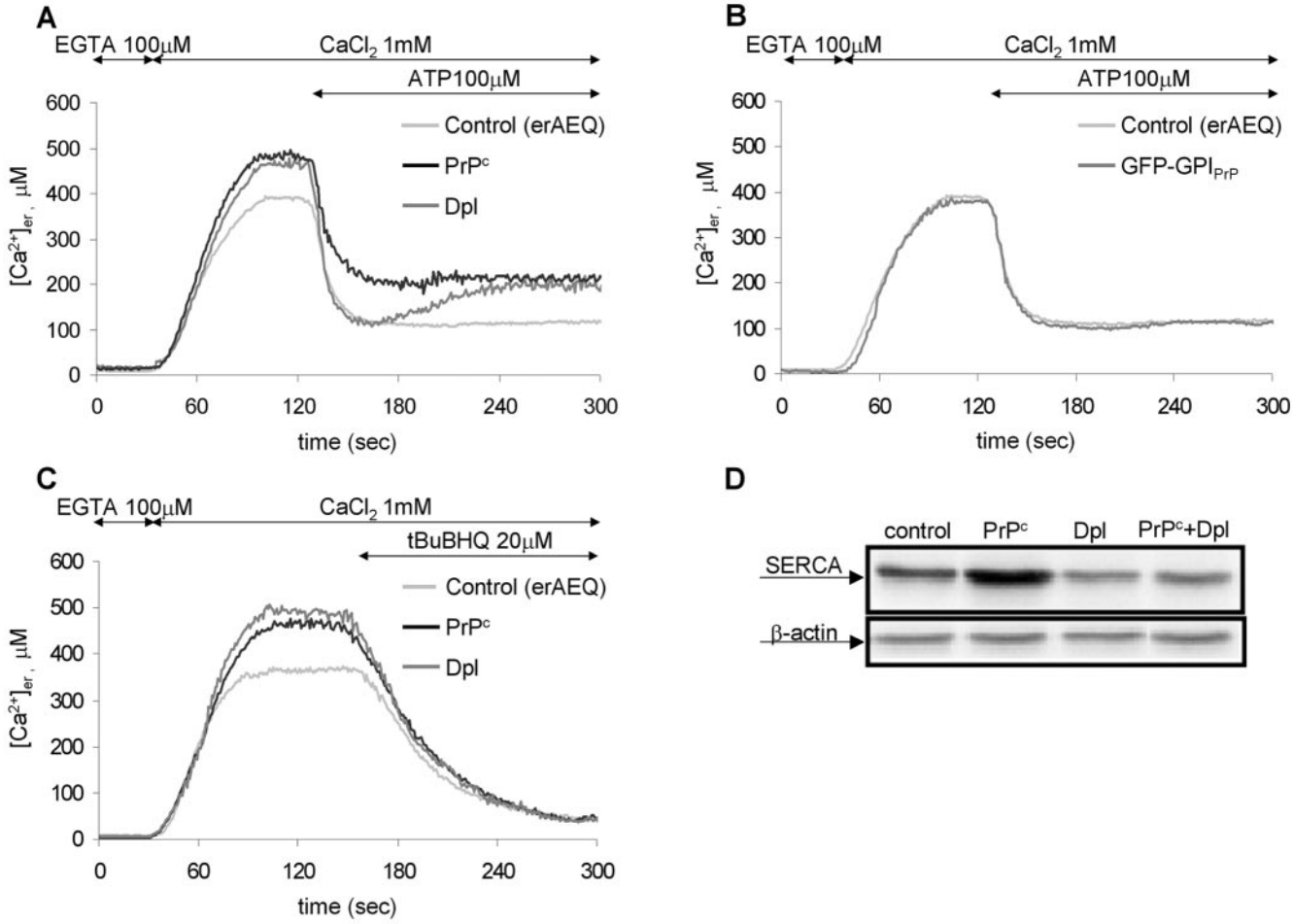

Figure 2. Effects of the presence of PrP^c or Dpl (A), and of GFP-GPI_{PrP} (B), on the Ca^{2+} filling of the ER lumen and on the agonist-stimulated ER Ca^{2+} discharge, and effects of the presence of PrP^c, or/and Dpl, on the ER membrane Ca^{2+} passive efflux (C), and SERCA expression (D). (A–C) CHO cells, transiently expressing erAEQ alone (control, light gray trace), or together with PrP^c (black trace) or Dpl (dark gray trace; A and C), or GFP-GPI_{PrP} (dark gray trace; B), were first depleted of Ca^{2+} (see *Materials and Methods* and text) and then incubated with 5 μM coelenterazine n (in EGTA-supplemented KRB), and finally, after extensive washings, transferred to the thermostatted chamber of the luminometer and perfused with EGTA-containing KRB. As monitored by erAEQ, EGTA replacement by $CaCl_2$ (1 mM) at the indicated time points induced the Ca^{2+} accumulation into the ER lumen, whereas addition of $InsP_3$-generating agonist ATP (100 μM; A and B), or of the SERCA inhibitor, tBuBHQ (20 μM; C), stimulated the ion discharge. Note that, although cells with either PrP^c or Dpl maintained a similar resting $[Ca^{2+}]_{er}$ (by ~15% higher than in controls; A and C), ATP-induced Ca^{2+} efflux from the ER was more extensive in Dpl-containing cells (A), followed by a partial refilling of ER stores. Conversely, the levels of resting and discharged $[Ca^{2+}]_{er}$ in cells with GFP-GPI_{PrP} were as in the control (B). When cells were challenged with tBuBHQ, no difference was observed in the ER membrane passive permeability of the three cell types (C). Presented data are typical of at least seven independent experiments, which yielded equivalent results. (D) Western blots of the endogenous SERCA and β-actin in controls (first lane) or in cells expressing PrP^c (second lane) and Dpl (third lane) separately, or together (fourth lane), using mAbs against the ubiquitous SERCA 2 isoform and β-actin, respectively. By normalizing the density of each SERCA band to the corresponding β-actin band, cells with PrP^c resulted to express the highest, and those expressing Dpl (alone or together with PrP^c) the lowest, quantity of SERCA.

the passive permeability of the ER membrane, at least judging from the similar response (in terms of both kinetics and amplitude) in PrP^c- and Dpl-containing cells to the addition of 2,5-di-(*tert*-butyl)-1,4-benzohydroquinone (tBuBHQ), an inhibitor of the ER Ca^{2+} pump (Kass *et al.*, 1989; Figure 2C). After the demonstration that IP_3-sensitive stores are fully depleted by inhibiting ER Ca^{2+} ATPases (Vanoevelen *et al.*, 2004), these data also suggest that the larger Ca^{2+} amounts accumulated by cells with PrP^c (or Dpl), and the smaller IP_3-induced Ca^{2+} efflux by cells expressing PrP^c (shown in Figure 2A), are not due to the recruitment of IP_3-insensitive Ca^{2+} compartments. This conclusion is further corroborated by the finding that, when pretreating control, and PrP^c-expressing, cells with thapsigargin (an irreversible SERCA inhibitor; Thastrup *et al.*, 1990), in both cases the uptake of Ca^{2+} in the ER was <10% of the maximal quantity observed in thapsigargin-untreated controls (unpublished data; see also Brini *et al.*, 2000). We could also exclude that data with PrP^c are biased by the mode of transfection, or the protein quantity, in that the effects of the protein on the ER Ca^{2+} handling are reproduced in PrP^c-stably transfected CHO cells, which express the protein in lower amounts (unpublished data). Unfortunately, analysis of stably expressed Dpl molecules could not be carried out, given the impossibility, under our conditions, to establish viable clones with CHO cells.

We then examined whether the presence of PrP^c and Dpl affected the expression of ER proteins such as SERCA or

calreticulin. The latter protein is not only crucial for the ER Ca^{2+}-buffering capacity (Krause and Michalak, 1997), but can also regulate $InsP_3Rs$ (Arnaudeau *et al.*, 2002). We could not attribute to calreticulin the different modes of Ca^{2+} efflux from the ER, because the three cell types expressed the protein at similar levels (unpublished data). However, with respect to controls, we found higher and lower SERCA amounts in the presence of PrP^c and Dpl, respectively (Figure 2D, lanes 1–3). Possibly, PrP^c and Dpl trigger a signal that interferes with the expression of the protein in an opposed way.

Cytosolic Ca^{2+} in PrP^c- or Dpl-expressing Cells

Having found that the presence of PrP^c, or Dpl, affects the Ca^{2+} handling of the main intracellular Ca^{2+} store, we then set out to evaluate if and how the proteins influenced cytosolic Ca^{2+} concentration ($[Ca^{2+}]_c$) under resting conditions, or after cell stimulation. AEQ steep response curve precludes the accurate estimation of $[Ca^{2+}]$ lower than 200–300 nM (Brini *et al.*, 1995), a concentration typical of the cytosol of resting cells. This parameter was therefore determined through the image analysis of single cells loaded with the fluorescent Ca^{2+} indicator fura-2, after identifying successfully transfected cells by the coexpression of GFP (Brini *et al.*, 1995). We found that fura-2 signals (given by the ratio of fluorescence emitted by illuminating cells at 340 and 380 nm) detected in PrP^c- or Dpl-expressing cells have a magnitude similar to that of the control (Figure 3A), suggesting that no appreciable alteration in basal $[Ca^{2+}]_c$ is attributable to these proteins.

Conversely, cytAEQ was used to monitor changes in $[Ca^{2+}]_c$ after the cell stimulation by ATP. As shown (Figure 3B), addition of the agonist to cells induced a similar rise of $[Ca^{2+}]_c$ in both control cells (light gray trace; 3.9 ± 0.4 μM, n = 19) and in those expressing Dpl (dark gray trace; 3.9 ± 0.3 μM, n = 17), whereas in cells with PrP^c a statistically significant reduction of the Ca^{2+} transient was observed (black trace; 3.4 ± 0.4 μM, n = 18). It is to be noted, however, that under the used conditions two processes contribute to elevating $[Ca^{2+}]_c$; one is the $InsP_3$-induced discharge of ER Ca^{2+} stores; the other is the Ca^{2+} influx from the extracellular space through the so-called capacitative Ca^{2+} entry (CCE), which becomes activated by a retrograde signal arising from the ER Ca^{2+} depletion (Putney *et al.*, 2001). Hence, to dissect the contribution of each individual process, cells were subjected to a time-based protocol. First, adding ATP to cells placed in a Ca^{2+}-free medium induced Ca^{2+} efflux from the ER (Figure 3C). As shown, we found an identical peak transient in control cells (light gray trace; 2.7 ± 0.6 μM, n = 12) and in those with Dpl (dark gray trace; 2.7 ± 0.3 μM, n = 14), whereas a reduced value was again observed in cells with PrP^c (black trace; 2.1 ± 0.3 μM, n = 12). After the transients subsided, cells were exposed to a 1 mM $CaCl_2$-containing medium. This caused a second peak, as expected from CCE through activated store-operated Ca^{2+} channels (SOCC). In this case, however, no statistically significant difference was evident in the three cell types (0.92 ± 0.13 μM, n = 10 in control cells; 0.80 ± 0.09 μM, n = 7, in cells with Dpl; 0.89 ± 0.14 μM, n = 8, in cells with PrP^c). Similar results were obtained with fura-2 (unpublished data).

Subplasma Membrane Ca^{2+} Pools in PrP^c- or Dpl-expressing Cells

pmAEQ, which targets to the cytosolic rim of the plasma membrane (Marsault *et al.*, 1997), was used to monitoring the Ca^{2+} concentration in these restricted cytosolic domains ($[Ca^{2+}]_{pm}$; Figure 4). ATP addition to cells in the presence of 1 mM $CaCl_2$ (panel A) resulted in transient $[Ca^{2+}]_{pm}$ rises of similar magnitude in controls (light gray trace; 4.7 ± 0.8 μM, n = 12) and in Dpl-expressing cells (dark gray trace; 5.3 ± 1.5 μM, n = 9), in contrast to the almost eightfold higher $[Ca^{2+}]_{pm}$ peak found in those housing PrP^c (black trace; 42 ± 12 μM, n = 7). After the reestablishment of resting conditions, cells with PrP^c continued to maintain a statistically significant enhanced $[Ca^{2+}]_{pm}$ value (1.9 ± 0.6 μM, n = 6) than in controls (0.90 ± 0.20 μM, n = 10), although also in the presence of Dpl the basal $[Ca^{2+}]_{pm}$ remained at a higher level (1.5 ± 0.4 μM, n = 7; see inset to the figure). As reported in panel B, a similar influence of PrP^c and Dpl on $[Ca^{2+}]_{pm}$ was evident when CCE was alternatively activated by adding $CaCl_2$ (1 mM) to Ca^{2+}-depleted cells (peak and steady state values were, respectively, 40 ± 12 μM, n = 11 and 6.2 ± 2.7 μM, n = 7, in cells with PrP^c; 24 ± 7 μM, n = 11 and 4.5 ± 0.9 μM, n = 8, in cells with Dpl; and 22 ± 8 μM, n = 7 and 2.9 ± 0.7 μM, n = 6, in controls). Altogether, these results suggest that the recombinant expression of PrP^c strongly increases Ca^{2+} entry from the extracellular space, whereas the attenuated effect by Dpl becomes evident only under steady state conditions.

Mitochondrial Ca^{2+} in PrP^c- or Dpl-expressing Cells

Compelling evidence indicates that in several cell types, including CHO cells, mitochondria behave as reporters of localized Ca^{2+} changes originating from the stimulation of the $InsP_3Rs$, in that the Ca^{2+} rise at the channels' mouth triggers the activity of the low-affinity Ca^{2+} uniporter of mitochondria juxtaposed to $InsP_3Rs$ (Rizzuto *et al.*, 1998). Such a spatial link between the two organelles, which according to recent data may also involve stable physical interactions (Filippin *et al.*, 2003), ensures that mitochondria receive ER signals with maximal efficiency. To examine the influence of PrP^c and Dpl on such mechanism, we used mtAEQ targeted to the mitochondrial matrix (Rizzuto *et al.*, 1992; Montero *et al.*, 2000). Intriguingly, ATP addition resulted in a mitochondrial Ca^{2+} signal ($[Ca^{2+}]_m$) that was specific for each case (Figure 5); cells with PrP^c showed the lowest value (black trace; 42 ± 11 μM, n = 9), the control ones the intermediate value (light gray trace; 62 ± 15 μM, n = 7), whereas the highest Ca^{2+} accumulation was detected in the presence of Dpl (dark gray trace; 110 ± 15 μM, n = 10). In the latter case, the average $[Ca^{2+}]_m$ value was more than twice that occurring with PrP^c. Therefore, in line with the close coupling between quantity of Ca^{2+} released from the ER and Ca^{2+} amounts accumulated by mitochondria, these data emphasize the findings on the ER Ca^{2+} discharge monitored by erAEQ (see Figure 2A).

Coexpression of PrP^c and Dpl Abolishes the Divergent Effects on Ca^{2+} Signaling Observed in Cells Expressing PrP^c, or Dpl, Alone

In view of the opposite effects on local Ca^{2+} fluctuations elicited by PrP^c and Dpl reported here and of the functional interplay of the two proteins suggested by genetic approaches (Kuwahara *et al.*, 1999; Moore *et al.*, 2001; Rossi *et al.*, 2001; Yamaguchi *et al.*, 2004), one expects that the Ca^{2+} signals observed in cells expressing PrP^c and Dpl separately will be modified by the copresence of the proteins in the same cell. To verify this assumption, we monitored Ca^{2+} homeostasis in the various compartments of cells transiently cotransfected with PrP^c and Dpl, after controlling that the two proteins are expressed at levels comparable to those found in singly transfected cells (Figure 1B, third lanes; note that, irrespective of the used plasmid batch(es), the transfection efficiency was generally ~35%). Indeed, we found that

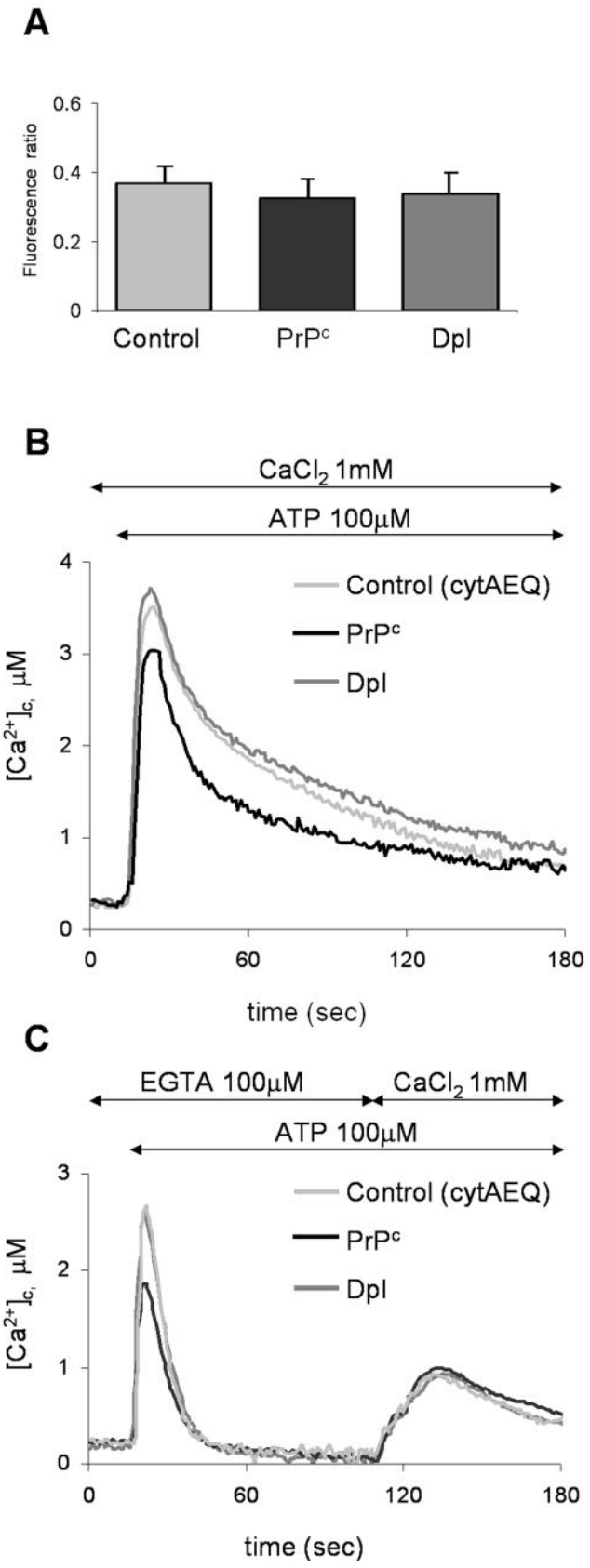

Figure 3. Resting $[Ca^{2+}]_c$ (A) and ATP-induced effects on $[Ca^{2+}]_c$ (B and C), in CHO cells transiently expressing cytAEQ alone (control), or together with PrP^c, or Dpl. (A) Resting $[Ca^{2+}]_c$, monitored by the Ca^{2+}-indicator fura-2, is expressed as the ratio of the fluorescence emitted by fura-2 after cell excitation at 340 and 380 nm (see *Materials and Methods*). No statistically significant difference was found in the three cell types. (B) $[Ca^{2+}]_c$ transients, after ATP (100 μM) addition at the indicated time point, were monitored with cytAEQ reconstituted with wild-type coelenterazine (5 μM; see *Materials and Methods*). Although a similar peak was found in controls (light gray trace) and Dpl-containing cells (dark gray trace), cells with PrP^c (black trace) gave rise to a transient of smaller magnitude. (C) Using the above described cytAEQ, a protocol was applied so as to evaluate the contribution to the ATP-induced $[Ca^{2+}]_c$ movements shown in B, first of the $InsP_3$-induced Ca^{2+} mobilization (first peak, ATP added in the presence of 100 μM EGTA, i.e., with no external Ca^{2+}) and then of the Ca^{2+} influx from the external medium (second peak, in the presence of 1 mM $CaCl_2$). On Ca^{2+} release from the ER (first peak), a transient of smaller magnitude was again observed in cells with PrP^c, whereas no difference in the second peak was evident in the three cell types. Presented data are typical of at least seven independent experiments, which yielded equivalent results.

under this condition local Ca^{2+} signals are extremely close to those of control cells (Figure 6), but for the ER Ca^{2+} efflux rate (panel A) that after PrP^c and Dpl cotransfection is faster than in controls by around 30% ($V_{1/2}$ being 33 $\pm$ 3 μM/s, n = 6, in cotransfected cells; 23 $\pm$ 4 μM/s, n = 5, in controls). It is interesting to note that a similar percentage difference is also found when comparing the corresponding $V_{1/2}$ values of controls and Dpl-expressing cells (Figure 2A, and text), and that cells transfected with Dpl, either alone or together with PrP^c, present the lowest amounts of SERCA (third and fourth lanes of Figure 2D).

DISCUSSION

Several reports indicate that reduction of PrP^c functionality causes perturbations in Ca^{2+} signaling and that the provoked alteration in some plasma membrane currents may explain aspects of TSEs, including a few neurologic symptoms (Cathala and Baron, 1987) and loss of neurons (Gray *et al.*, 1999). On this background, we examined whether PrP^c takes part in the complex mechanism that controls Ca^{2+} homeostasis by analyzing, for the first time, Ca^{2+} fluctuations in different compartments of cells transfected with PrP^c and recombinant targeted aequorins. We found that the way cells with PrP^c handle compartmentalized Ca^{2+} favors the cell protective role attributed to PrP^c, in contrast with the effects arising from the presence of Dpl. Such a divergent activity, and the capacity of PrP^c—cotransfected with Dpl—to suppress the effects elicited by Dpl alone, highlights the protective function of PrP^c N-domain (absent from Dpl), as also deduced from experiments with cells challenged by serum deprivation (Sakudo *et al.*, 2003) or over expressing toxic PrP fragments (Shmerling *et al.*, 1998), proapoptotic Bax (Bounhar *et al.*, 2001), or Dpl itself (Atarashi *et al.*, 2003).

The most remarkable features observed in PrP^c-containing cells regard $[Ca^{2+}]_{pm}$ pools and the ER-mitochondria Ca^{2+} coupling. In considering the highest $[Ca^{2+}]_{pm}$ found in the presence of PrP^c (Figure 4), the simplest explanation is that PrP^c activates SOCCs. This is important, in view of the suggestion that the capacitative entry of Ca^{2+} in neuronal cells may serve in signaling pathways, not only in the refilling of Ca^{2+} stores observed in nonexcitable cells, and that subplasma membrane Ca^{2+}-rich domains may trigger key physiological cell events (Putney, 2003). For example, SOCCs can be functionally coupled with adenylyl cyclase (Fagan *et al.*, 2000); PrP^c-elicited $[Ca^{2+}]_{pm}$ rises may thus

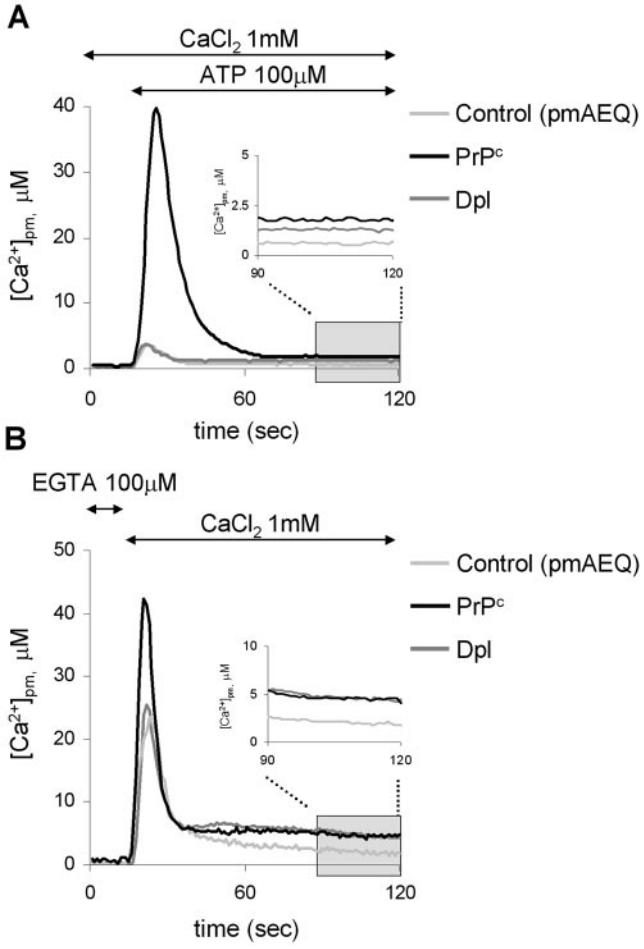

Figure 4. Monitoring the subplasma membrane Ca^{2+} concentration with pmAEQ. (A) Response to ATP (100 μM) of CHO cells transiently expressing pmAEQ alone (control, light gray trace), or together with PrP^c (black trace) or Dpl (dark gray trace), and maintained in 1 mM $CaCl_2$. pmAEQ was reconstituted by incubating cells with wild-type coelenterazine (5 μM; see *Materials and Methods*). Addition of ATP provoked a $[Ca^{2+}]_{pm}$ transient that in cells with PrP^c was by far more elevated than in the other two cell types. With respect to the control, however, the resting $[Ca^{2+}]_{pm}$ level remained significantly higher in the presence of both PrP^c and Dpl (in the inset, resting $[Ca^{2+}]_{pm}$ are reported on an expanded scale). (B) Response to $CaCl_2$ addition (1 mM) in the same cell types described in A, but maintained in (Ca^{2+}-free) KRB supplemented with EGTA (100 μM). After pmAEQ reconstitution, addition of 1 mM $CaCl_2$ induced a response that mimicked that shown in A with respect to both peak and resting $[Ca^{2+}]_{pm}$ levels. The latter are also shown in the inset on an expanded scale. Presented data are typical of at least six independent experiments, which yielded equivalent results.

represent the so-far missing intermediate linking the activation of cytosolic cAMP-dependent protein kinase A by cell surface-attached PrP^{c}s, which was shown to inhibit apoptosis in retinal explants (Chiarini *et al.*, 2002). Also, in analogy with SOCCs modulation of transmitter release and synaptic plasticity in certain neurons (Emptage *et al.*, 2001), PrP^c-elicited Ca^{2+} hotspots may recruit effectors in the immediate vicinity, e.g., Ca^{2+}-activated K^+ channels, thereby explaining why impairment of (Ca^{2+}-dependent) K^+ currents in PrP-null cells could not be attributed to specific alterations of voltage-gated Ca^{2+} channels (Herms *et al.*, 2000; but see Whatley *et al.*, 1995). In the light of all these considerations, it is thus tempting to speculate that, as observed in the used cell model system, PrP^c affects SOCC-dependent subplasma membrane Ca^{2+} pools also in neurons. If this were the case, impairment of SOCCs could play a major role in TSE neurologic manifestations (Cathala and Baron, 1987).

Equally important is the way by which PrP^c-expressing cells control ER and mitochondrial Ca^{2+} homeostases, either of which is crucial in cell survival. Indeed, $[Ca^{2+}]_{er}$ variations may trigger stress responses, whereas substantial ER Ca^{2+} discharges may increase mitochondrial Ca^{2+} levels that, by activating caspase-9, a member of the death-specific caspase family (Cryns and Yuan, 1998), determine the pathway leading to apoptotic death (Li *et al.*, 1997). Hence, despite the potentially dangerous elevated $[Ca^{2+}]_{er}$ (Pinton *et al.*, 2000, 2001), our demonstration that the presence of PrP^c limits the agonist-stimulated ER Ca^{2+} release (Figures 2A and 3C) and, most importantly, the ion accumulation by mitochondria (Figure 5), is not only consistent with a PrP^c protective role, but it also predicts an increased cell vulnerability upon reducing PrP^c molecules, and/or expression of TSE-associated PrP mutants that accumulate in the ER (Singh *et al.*, 1997; Zanusso *et al.*, 1999; Jin *et al.*, 2000; Negro *et al.*, 2001). Accordingly, one of the first events observed in neuronal cells exposed to purified PrP^{Sc} is a substantial ER Ca^{2+} discharge, followed by up-regulation of stress proteins and activation of the ER-resident caspase-12 that acts on other effector caspases to produce apoptosis (Hetz *et al.*, 2003b).

Conversely, stimulation of Dpl-expressing cells leads to a more pronounced and faster efflux of ER Ca^{2+} (Figure 2A) and to a large rise in $[Ca^{2+}]_m$ (Figure 5). These results, collected in the absence of apoptotic stimuli, disclose a possible mechanism by which Dpl sensitizes cells to environmental insults, whereas the difficulty in obtaining neuroblastoma (Massimino *et al.*, 2004), or CHO (this article), clones with Dpl suggests that the intrinsic toxicity of Dpl may manifest in cells other than Purkinje cells, the prime target of

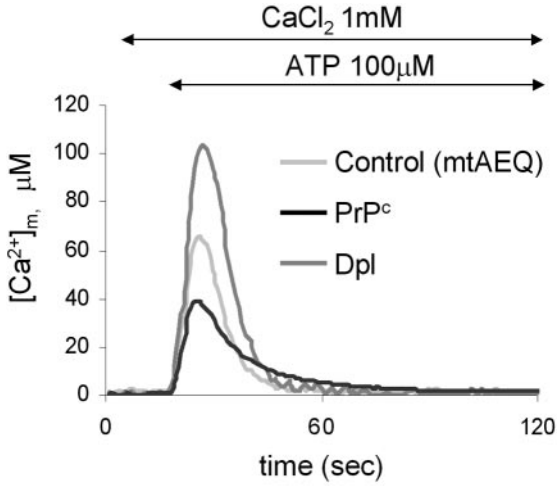

Figure 5. ATP-induced effects on $[Ca^{2+}]_m$ in CHO cells transiently expressing mtAEQ alone (control, light gray trace), or together with PrP^c (black trace) or Dpl (dark gray trace). mtAEQ was reconstituted by incubating cells with wild-type coelenterazine (5 μM; see *Materials and Methods*). The addition of ATP (100 μM) induced a rise in the $[Ca^{2+}]_m$ that was higher in Dpl-expressing cells than in the other two cell types. Presented data are typical of at least seven independent experiments, which yielded equivalent results.

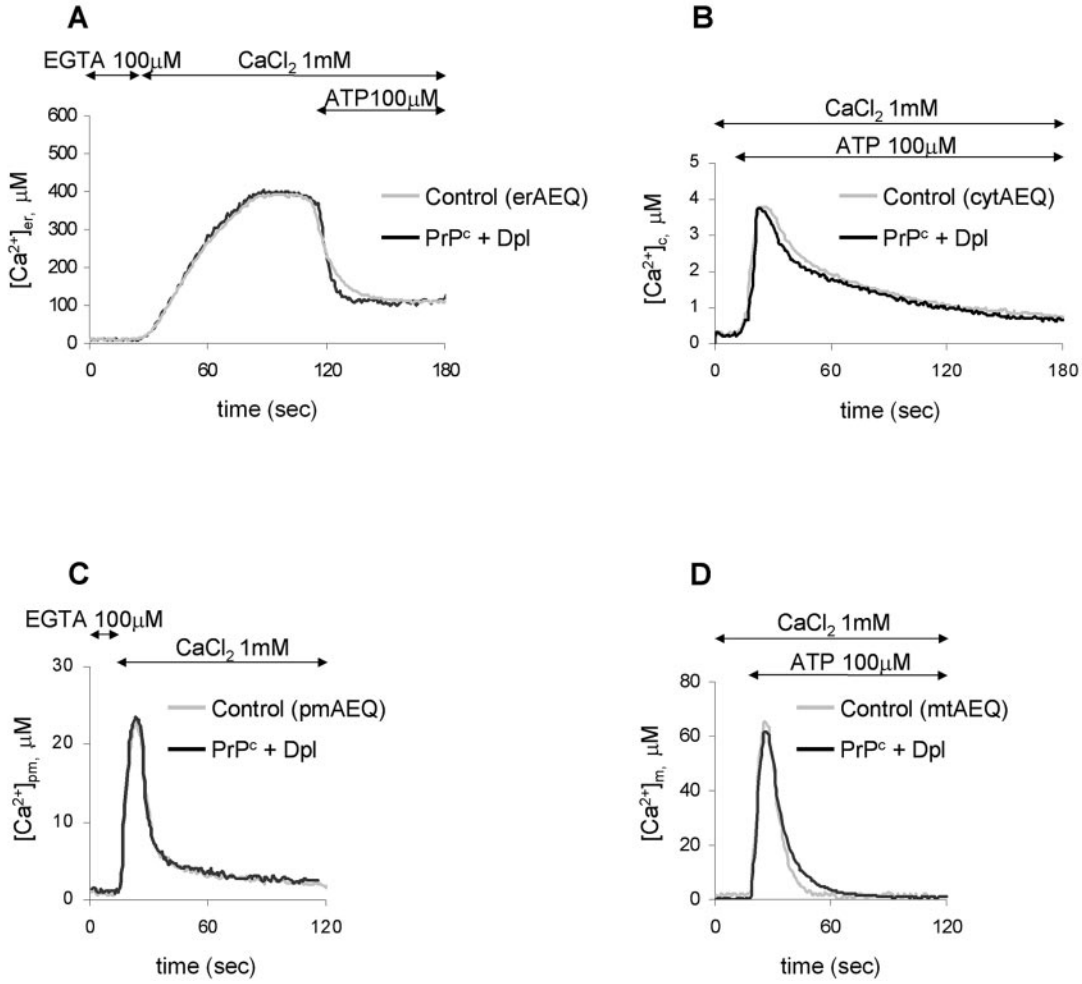

Figure 6. Monitoring $[Ca^{2+}]_{er}$ (A), $[Ca^{2+}]_c$ (B), $[Ca^{2+}]_{pm}$ (C), and $[Ca^{2+}]_m$ (D) in CHO cells transiently expressing the corresponding AEQ alone (control, light gray trace), or together with both PrP^c and Dpl (black trace). Experimental conditions were as reported in the legend to Figures 2A, 3B, 4B, and 5, respectively. Clearly, the copresence of PrP^c and Dpl abolished the divergent Ca^{2+} signaling observed in the various compartments of cells expressing PrP^c, or Dpl, alone. Presented data are typical of at least nine independent experiments, which yielded equivalent results.

Dpl pathogenicity (Sakaguchi *et al.*, 1996). Interestingly, biochemical analyses of Dpl-over-expressing brain tissues have proposed that the protein toxicity relates to an increased oxidative damage, possibly linked to impaired copper metabolism (Wong *et al.*, 2001). These data well agree with the demonstration that, despite the capacity of Dpl to bind copper like the related PrP^c C-terminus, different structural and functional roles pertain to Dpl- and PrP^c-bound coppers (Cereghetti *et al.*, 2004; see also Sakudo *et al.*, 2004). However, it seems also consistent with the influence of Dpl on mitochondrial Ca^{2+} handling reported here, given that deregulation of the organelle Ca^{2+} homeostasis can lead to the overproduction of toxic reactive oxygen species (Toescu and Verkhratsky, 2003).

As for the divergent ER Ca^{2+} handling, we found that cells with PrP^c and Dpl express higher and lower amounts of SERCA, respectively, than control cells (Figure 2D). This data may explain why, irrespective of an identical Ca^{2+} load, the balance between $InsP_3R$-mediated Ca^{2+} efflux from, and SERCA-mediated Ca^{2+} (re-)loading in, the ER results in a less pronounced net Ca^{2+} discharge with PrP^c than with Dpl (Figure 2A). ER Ca^{2+} load, however, depends on both the amount and activity of the SERCA pumps. We have shown that in cells with Dpl CCE generates steady state $[Ca^{2+}]_{pm}$ levels higher than in controls (Figure 4). It seems therefore possible to hypothesize that, in line with other observations (Mogami *et al.*, 1997), $[Ca^{2+}]_{pm}$ in Dpl-expressing cells stimulates the SERCA activity, thus explaining why, despite lower SERCA amounts, also these cells maintain a higher resting $[Ca^{2+}]_{er}$ than in controls (Figure 2A). Likewise, $[Ca^{2+}]_{pm}$ may also account for the slow refilling of ER stores occurring after the agonist-induced maximal Ca^{2+} depletion (Figure 2A). An important support to the key role of $[Ca^{2+}]_{pm}$ magnitude in regulating ER Ca^{2+} handling comes from cells housing PrP^c and Dpl together; they display low SERCA levels as well as low $[Ca^{2+}]_{pm}$ and are unable to exhibit the same $[Ca^{2+}]_{er}$ features observed in cells with Dpl alone (Figure 6).

In accord with the suggested functional interrelationship of the proteins, PrP^c and Dpl copresence abolishes Dpl effects on local Ca^{2+} movements (Figure 6). Several hypotheses have been suggested to explain PrP^c protection against Dpl (Behrens and Aguzzi, 2002): that PrP^c and Dpl compete for a common ligand (in the absence of PrP^c, the binding of

Dpl to the ligand would elicit an apoptotic signal); that PrP^c antagonizes an independent action of Dpl that sensitizes neurons to apoptosis (PrP-null cells would no longer control oxidative stress and Dpl deleterious function would predominate); and that PrP^c interferes with unselective multimeric pores formed by Dpl in the ER and/or plasma membrane. With respect to the latter hypothesis, the similar passive ER Ca^{2+} efflux in PrP^c- or Dpl-expressing cells (Figure 2C) implies that Dpl is unlikely to form (Ca^{2+}) leak pathways in the ER membrane. On the other hand, the Ca^{2+} handling in cells expressing PrP^c and Dpl together closely matches that of control cells (Figure 6), not that observed in the presence of PrP^c alone. A possible interpretation for such a balanced effect entails that, at least in CHO cells, PrP^c and Dpl have independent, opposite activities, rather than the capacity to competing for a common ligand.

In conclusion, we have shown that the recombinantly expressed PrP^c governs the cell Ca^{2+} metabolism in a cell-protective manner, by limiting the Ca^{2+} accumulation into mitochondria. Yet, PrP^c consistently increases $[Ca^{2+}]_{pm}$, suggesting that these elevated Ca^{2+} pools may contribute to regulating the (Ca^{2+}-dependent) cell excitability and/or PrP^c-mediated signaling, either of which is critical for neuronal survival.

ACKNOWLEDGMENTS

M.B. acknowledges funding from the Ministero dell'Istruzione, dell'Università e della Ricerca (MUIR) (PRIN 2003), and M.C.S. from the European Union (BioMed.2 BMH4-CT98–6050), Telethon Onlus (E.0945), MIUR (PRIN 2004 and RBNE01S29H), and the Italian Ministry of Health (1AA/F, 2001).

REFERENCES

Arnaudeau, S., Frieden, M., Nakamura, K., Castelbou, C., Michalak, M., and Demaurex, N. (2002). Calreticulin differentially modulates calcium uptake and release in the endoplasmic reticulum and mitochondria. J. Biol. Chem. *277*, 46696–46705.

Atarashi, R., Nishida, N., Shigematsu, K., Goto, S., Kondo, T., Sakaguchi, S., and Katamine, S. (2003). Deletion of N-terminal residues 23–88 from prion protein (PrP) abrogates the potential to rescue PrP-deficient mice from PrP-like protein/doppel-induced neurodegeneration. J. Biol. Chem. *278*, 28944–28949.

Barrero, M. J., Montero, M., and Alvarez, J. (1997). Dynamics of [Ca^{2+}] in the endoplasmic reticulum and cytoplasm of intact HeLa cells: a comparative study. J. Biol. Chem. *272*, 27694–27699.

Barrow, P. A., Holmgren, C. D., Tapper, A. J., and Jefferys, J. G. (1999). Intrinsic physiological and morphological properties of principal cells of the hippocampus and neocortex in hamsters infected with scrapie. Neurobiol. Dis. *6*, 406–423.

Behrens, A., and Aguzzi, A. (2002). Small is not beautiful: antagonizing functions for the prion protein PrP(C) and its homologue Dpl. Trends Neurosci. *25*, 150–154.

Bernardi, P. (1999). Mitochondrial transport of cations: channels, exchangers, and permeability transition. Physiol. Rev. *79*, 1127–1155.

Bounhar, Y., Zhang, Y., Goodyer, C. G., and LeBlanc, A. (2001). Prion protein protects human neurons against Bax-mediated apoptosis. J. Biol. Chem. *276*, 39145–39149.

Brini, M. (2003). Ca^{2+} signalling in mitochondria: mechanism and role in physiology and pathology. Cell Calcium *34*, 399–405.

Brini, M., Bano, D., Manni, S., Rizzuto, R., and Carafoli, E. (2000). Effects of PMCA and SERCA pump overexpression on the kinetics of cell Ca^{2+} signalling. EMBO J *19*, 4926–4935.

Brini, M., Marsault, R., Bastianutto, C., Alvarez, J., Pozzan, T., and Rizzuto, R. (1995). Transfected aequorin in the measurement of cytosolic Ca^{2+} concentration ($[Ca^{2+}]_c$): a critical evaluation. J. Biol. Chem. *270*, 9896–9903.

Brown, D. R., Nicholas, R. S., and Canevari, L. (2002). Lack of prion protein expression results in a neuronal phenotype sensitive to stress. J. Neurosci. Res. *67*, 211–224.

Brown, D. R. *et al.* (1997). The cellular prion protein binds copper in vivo. Nature *390*, 684–687.

Bueler, H., Fischer, M., Lang, Y., Bluethmann, H., Lipp, H. P., DeArmond, S. J., Prusiner, S. B., Aguet, M., and Weissmann, C. (1992). Normal development and behaviour of mice lacking the neuronal cell-surface PrP protein. Nature *356*, 577–582.

Cathala, F., and Baron, H. (1987). Clinical aspects of Creutzfeldt–Jakob disease. In: Prions: Novel Infectious Pathogens Causing Scrapie and Creutzfeldt-Jakob Disease, ed. S. B. Prusiner and M. P. McKinley, San Diego: Academic Press, 467–509.

Cereghetti, G. M., Negro, A., Vinck, E., Massimino, M. L., Sorgato, M. C., and Van Doorslaer, S. (2004). Copper(II) binding to the human Doppel protein may mark its functional diversity from the prion protein. J. Biol. Chem. *279*, 36497–36503.

Chiarini, L. B., Freitas, A. R., Zanata, S. M., Brentani, R. R., Martins, V. R., and Linden, R. (2002). Cellular prion protein transduces neuroprotective signals. EMBO J. *21*, 3317–3326.

Colling, S. B., Collinge, J., and Jefferys, J. G. (1996). Hippocampal slices from prion protein null mice: disrupted Ca^{2+}-activated K^+ currents. Neurosci. Lett. *209*, 49–52.

Cryns, V., and Yuan, J. (1998). Proteases to die for. Genes Dev. *12*, 1551–1570.

Emptage, N. J., Reid, C. A., and Fine, A. (2001). Calcium stores in hippocampal synaptic boutons mediate short-term plasticity, store-operated Ca^{2+} entry, and spontaneous transmitter release. Neuron *29*, 197–208.

Fagan, K. A., Graf, R. A., Tolman, S., Schaack, J., and Cooper, D. M. (2000). Regulation of a Ca^{2+}-sensitive adenylyl cyclase in an excitable cell. Role of voltage-gated versus capacitative Ca^{2+} entry. J. Biol. Chem. *275*, 40187–40194.

Filippin, L., Magalhaes, P. J., Di Benedetto, G., Colella, M., and Pozzan, T. (2003). Stable interactions between mitochondria and endoplasmic reticulum allow rapid accumulation of calcium in a subpopulation of mitochondria. J. Biol. Chem. *278*, 39224–39234.

Gray, F., Chretien, F., Adle-Biassette, H., Dorandeu, A., Ereau, T., Delisle, M. B., Kopp, N., Ironside, J. W., and Vital, C. (1999). Neuronal apoptosis in Creutzfeldt-Jakob disease. J. Neuropathol. Exp. Neurol. *58*, 321–328.

Herms, J. W., Tings, T., Dunker, S., and Kretzschmar, H. A. (2001). Prion protein affects Ca^{2+}-activated K^+ currents in cerebellar Purkinje cells. Neurobiol. Dis. *8*, 324–330.

Herms, J. W., Korte, S., Gall, S., Schneider, I., Dunker, S., and Kretzschmar, H. A. (2000). Altered intracellular calcium homeostasis in cerebellar granule cells of prion protein-deficient mice. J. Neurochem. *75*, 1487–1492.

Hetz, C., Maundrell, K., and Soto, C. (2003a). Is loss of function of the prion protein the cause of prion disorders? Trends Mol. Med. *9*, 237–243.

Hetz, C., Russelakis-Carneiro, M., Maundrell, K., Castilla, J., and Soto, C. (2003b). Caspase-12 and endoplasmic reticulum stress mediate neurotoxicity of pathological prion protein. EMBO J. *22*, 5435–5445.

Jefferys, J. G., Empson, R. M., Whittington, M. A., and Prusiner, S. B. (1994). Scrapie infection of transgenic mice leads to network and intrinsic dysfunction of cortical and hippocampal neurones. Neurobiol. Dis. *1*, 25–30.

Jin, T., Gu, Y., Zanusso, G., Sy, M., Kumar, A., Cohen, M., Gambetti, P., and Singh, N. (2000). The chaperone protein BiP binds to a mutant prion protein and mediates its degradation by the proteasome. J. Biol. Chem. *275*, 38699–38704.

Johnston, A. R., Fraser, J. R., Jeffrey, M., and MacLeod, N. (1998). Synaptic plasticity in the CA1 area of the hippocampus of scrapie-infected mice. Neurobiol. Dis. *5*, 188–195.

Jouaville, L. S., Pinton, P., Bastianutto, C., Rutter, G. A., and Rizzuto, R. (1999). Regulation of mitochondrial ATP synthesis by calcium: evidence for a long-term metabolic priming. Proc. Natl. Acad. Sci. USA *96*, 13807–13812.

Kass, G.E.N., Dudd, S. K., Moore, G. A., and Orrenius, S. A. (1989). 2,5-Di(tert-butyl)-1,4-benzohydroquinone rapidly elevates cytosolic Ca^{2+} concentration by mobilizing the inositol 1,4,5-trisphosphate-sensitive Ca^{2+} pool. J. Biol. Chem. *264*, 15192–15198.

Krause, K. H., and Michalak, M. (1997). Calreticulin. Cell *88*, 439–443.

Kuwahara, C. *et al.* (1999). Prions prevent neuronal cell-line death. Nature *400*, 225–226.

Li, A., Sakaguchi, S., Shigematsu, K., Atarashi, R., Roy, B. C., Nakaoke, R., Arima, K., Okimura, N., Kopacek, J., and Katamine, S. (2000). Physiological expression of the gene for PrP-like protein, PrPLP/Dpl, by brain endothelial cells and its ectopic expression in neurons of PrP-deficient mice ataxic due to Purkinje cell degeneration. Am. J. Pathol. *157*, 1447–1452.

Li, P., Nijhawan, D., Budihardjo, I., Srinivasula, S. M., Ahmad, M., Alnemri, E. S., and Wang, X. (1997). Cytochrome c and dATP-dependent formation of

Apaf-1/caspase-9 complex initiates an apoptotic protease cascade. Cell *91*, 479–489.

Malgaroli, A., Milani, D., Meldolesi, J., and Pozzan, T. (1987). Fura-2 measurements of cytosolic free Ca^{2+} monolayers and suspensions of various cell types of animal cells. J. Cell Biol. *105*, 2145–2155.

Mallucci, G. R., Ratte, S., Asante, E. A., Linehan, J., Gowland, I., Jefferys, J. G., and Collinge, J. (2002). Post-natal knockout of prion protein alters hippocampal CA1 properties, but does not result in neurodegeneration. EMBO J. *21*, 202–210.

Manson, J. C., Clarke, A. R., Hooper, M. L., Aitchison, L., McConnell, I., and Hope, J. (1994). 129/Ola mice carrying a null mutation in PrP that abolishes mRNA production are developmentally normal. Mol. Neurobiol. *8*, 121–127.

Marsault, R., Murgia, M., Pozzan, T., and Rizzuto, R. (1997). Domains of high Ca^{2+} beneath the plasma membrane of living A7r5 cells. EMBO J. *16*, 1575–1581.

Massimino, M. L., Ballarin, C., Bertoli, A., Casonato, S., Genovesi, S., Negro, A., and Sorgato, M. C. (2004). Human Doppel and prion protein share common membrane microdomains and internalization pathways. Int. J. Biochem. Cell Biol. *36*, 2016–2031.

Mattson, M. P., LaFerla, F. M., Chan, S. L., Leissring, M. A., Shepel, P. N., and Geiger, J. D. (2000). Calcium signaling in the ER: its role in neuronal plasticity and neurodegenerative disorders. Trends Neurosci. *23*, 222–229.

Mo, H., Moore, R. C., Cohen, F. E., Westaway, D., Prusiner, S. B., Wright, P. E., and Dyson, H. J. (2001). Two different neurodegenerative diseases caused by proteins with similar structures. Proc. Natl. Acad. Sci. USA *98*, 2352–2357.

Mogami, H., Nakano, K., Tepikin, A. V., and Petersen, O. H. (1997). Ca^{2+} flow via tunnels in polarized cells: recharging of apical stores by focal Ca^{2+} entry through basal membrane patch. Cell *88*, 49–55.

Montero, M., Brini, M., Marsault, R., Alvarez, J., Sitia, R., Pozzan, T., and Rizzuto, R. (1995). Monitoring dynamic changes in free Ca^{2+} concentration in the endoplasmic reticulum of intact cells. EMBO J. *14*, 5467–5475.

Montero, M., Alonso, M. T., Carnicero, E., Cuchillo-Ibanez, I., Albillos, A., Garcia, A. C., Garcia-Sancho, J,. and Alvarez, J. (2000). Chromaffin-cell stimulation triggers fast millimolar mitochondrial Ca^{2+} transients that modulate secretion. Nat. Cell. Biol. *2*, 57–61.

Moore, R. C., Mastrangelo, P., Bouzamondo, E., Heinrich, C., Legname, G., Prusiner, S. B., Hood, L., Westaway, D., DeArmond, S. J., and Tremblay, P. (2001). Doppel-induced cerebellar degeneration in transgenic mice. Proc. Natl. Acad. Sci. USA *98*, 15288–15293.

Moore, R. C. *et al.* (1999). Ataxia in prion protein (PrP)-deficient mice is associated with upregulation of the novel PrP-like protein doppel. J. Mol. Biol. *292*, 797–817.

Nakagawa, T., Zhu, H., Morishima, N., Li, E., Xu, J., Yankner, B. A., and Yuan, J. (2000). Caspase-12 mediates endoplasmic-reticulum-specific apoptosis and cytotoxicity by amyloid-beta. Nature *403*, 98–103.

Negro, A., Ballarin, C., Bertoli, A., Massimino, M. L., and Sorgato, M. C. (2001). The metabolism and imaging in live cells of the bovine prion protein in its native form or carrying single amino acid substitutions. Mol. Cell Neurosci. *17*, 521–538.

Negro, A., Meggio, F., Bertoli, A., Battistutta, R., Sorgato, M. C., and Pinna, L. A. (2000). Susceptibility of the prion protein to enzymic phosphorylation. Biochem. Biophys. Res. Commun. *271*, 337–341.

Orrenius, S., Zhivotovsky, B., and Nicotera, P. (2003). Regulation of cell death: the calcium-apoptosis link. Nat. Rev. Mol. Cell. Biol. *4*, 552–565.

Paschen, W. (2001). Dependence of vital cell function on endoplasmic reticulum calcium levels: implications for the mechanisms underlying neuronal cell injury in different pathological states. Cell Calcium *29*, 1–11.

Pinton, P., Ferrari, D., Rapizzi, E., Di Virgilio, F., Pozzan, T., and Rizzuto, R. (2001). The Ca^{2+} concentration of the endoplasmic reticulum is a key determinant of ceramide-induced apoptosis: significance for the molecular mechanism of Bcl-2 action. EMBO J. *20*, 2690–2701.

Pinton, P., Ferrari, D., Magalhaes, P., Schulze-Osthoff, K., Di Virgilio, F., Pozzan, T., and Rizzuto, R. (2000). Reduced loading of intracellular Ca^{2+} stores and downregulation of capacitative Ca^{2+} influx in Bcl-2-overexpressing cells. J. Cell Biol. *148*, 857–862.

Prusiner, S. B. (1998). Prions. Proc. Natl. Acad. Sci. USA *95*, 13363–13383.

Putney, J. W., Jr. (2003). Capacitative calcium entry in the nervous system. Cell Calcium *34*, 339–344.

Putney, J. W., Jr., Broad, L. M., Braun, F. J., Lievremont, J. P., and Bird, G. S. (2001). Mechanisms of capacitative calcium entry. J. Cell Sci. *114*, 2223–2229.

Rizzuto, R., Simpson, A.W.M., Brini, M., and Pozzan, T. (1992). Rapid changes of mitochondrial Ca^{2+} revealed by specifically targeted recombinant aequorin. Nature *358*, 325–328.

Rizzuto, R., Brini, M., Bastianutto, C., Marsault, R., and Pozzan, T. (1995). Photoprotein-mediated measurement of calcium ion concentration in mitochondria of living cells. Methods Enzymol. *260*, 417–428.

Rizzuto, R., Pinton, P., Carrington, W., Fay, F. S., Fogarty, K. E., Lifshitz, L. M., Tuft, R. A., and Pozzan, T. (1998). Close contacts with the endoplasmic reticulum as determinants of mitochondrial Ca^{2+} responses. Science *280*, 1763–1766.

Rossi, D., Cozzio, A., Flechsig, E., Klein, M. A., Rulicke, T., Aguzzi, A., and Weissmann, C. (2001). Onset of ataxia and Purkinje cell loss in PrP null mice inversely correlated with Dpl level in brain. EMBO J. *20*, 694–702.

Sakaguchi, S. *et al.* (1996). Loss of cerebellar Purkinje cells in aged mice homozygous for a disrupted PrP gene. Nature *380*, 528–531.

Sakudo, A., Lee, D. C., Saeki, K., Nakamura, Y., Inoue, K., Matsumoto, Y., Itohara, S., and Onodera, T. (2003). Impairment of superoxide dismutase activation by N-terminally truncated prion protein (PrP) in PrP-deficient neuronal cell line. Biochem. Biophys. Res. Commun. *308*, 660–667.

Sakudo, A. *et al.* (2004). Prion protein suppresses perturbation of cellular copper homeostasis under oxidative conditions. Biochem. Biophys. Res. Commun. *313*, 850–855.

Shmerling, D. *et al.* (1998). Expression of amino-terminally truncated PrP in the mouse leading to ataxia and specific cerebellar lesions. Cell *93*, 203–214.

Silverman, G. L., Qin, K., Moore, R. C., Yang, Y., Mastrangelo, P., Tremblay, P., Prusiner, S. B., Cohen, F. E., and Westaway, D. (2000). Doppel is an N-glycosylated, glycosylphosphatidylinositol-anchored protein. Expression in testis and ectopic production in the brains of $Prnp^{0/0}$ mice predisposed to Purkinje cell loss. J. Biol. Chem. *275*, 26834–26842.

Singh, N., Zanusso, G., Chen, S. G., Fujioka, H., Richardson, S., Gambetti, P., and Petersen, R. B. (1997). Prion protein aggregation reverted by low temperature in transfected cells carrying a prion protein gene mutation. J. Biol. Chem. *272*, 28461–28470.

Streb, H., Irvine, R. F., Berridge, M. J., and Schulz, I. (1983). Release of Ca^{2+} from a nonmitochondrial intracellular store in pancreatic acinar cells by inositol-1,4,5-trisphosphate. Nature *306*, 67–69.

Thastrup, O., Cullen, P. J., Drobak, B. J., Hanley, M. R., and Dawson, A. P. (1990). Thapsigargin, a tumor promoter, discharges intracellular Ca2+ stores by specific inhibition of the endoplasmic reticulum Ca^{2+}-ATPase. Proc. Natl. Acad. Sci. USA *87*, 2466–2470.

Toescu, E. C., and Verkhratsky, A. (2003). Neuronal ageing from an intraneuronal perspective: roles of endoplasmic reticulum and mitochondria. Cell Calcium *34*, 311–323.

Vanoevelen, J., Raeymaekers, L., Parys, J. B., De Smedt, H., Van Baelen, K., Callewaert, G., Wuytack, F., and Missiaen, L. (2004). Inositol trisphosphate producing agonists do not mobilize the thapsigargin-insensitive part of the endoplasmic-reticulum and Golgi Ca^{2+} store. Cell Calcium *35*, 115–121.

Whatley, S. A., Powell, J. F., Politopoulou, G., Campbell, I. C., Brammer, M. J., and Percy, N. S. (1995). Regulation of intracellular free calcium levels by the cellular prion protein. Neuroreport *6*, 2333–2337.

Wong, B. S. *et al.* (2001). Induction of HO-1 and NOS in doppel-expressing mice devoid of PrP: implications for doppel function. Mol. Cell. Neurosci. *17*, 768–775.

Yamaguchi, N., Sakaguchi, S., Shigematsu, K., Okimura, N., and Katamine, S. (2004). Doppel-induced Purkinje cell death is stoichiometrically abrogated by prion protein. Biochem. Biophys. Res. Commun. *319*, 1247–1252.

Zanusso, G., Petersen, R. B., Jin, T., Jing, Y., Kanoush, R., Ferrari, S., Gambetti, P., and Singh, N. (1999). Proteasomal degradation and N-terminal protease resistance of the codon 145 mutant prion protein. J. Biol. Chem. *274*, 23396–23404.